Available online at www.sciencedirect.com
ScienceDirect
Trans. Nonferrous Met. Soc. China 29(2019) 1592−1600
Transactions of Nonferrous Metals Society of China
www.tnmsc.cn

Effects of La−Ce addition on microstructure and mechanical properties of Al−18Si−4Cu−0.5Mg alloy

Gao-yong LIN[1,2], Kun LI[1,2], Di FENG[3], Yong-ping FENG[4], Wei-yuan SONG[1,2], Meng-qiong XIAO[1,2]

1. School of Materials Science and Engineering, Central South University, Changsha 410083, China;
2. Key Laboratory of Nonferrous Metal Materials Science and Engineering, Ministry of Education, Central South University, Changsha 410083, China;
3. School of Materials Science and Engineering, Jiangsu University of Science and Technology, Zhenjiang 212000, China;
4. Fujian Xiangxin Shares Co., Ltd., Fuzhou 350000, China

Received 21 September 2018; accepted 11 April 2019

Abstract: The microstructural evolution and mechanical properties of Al−18Si−4Cu−0.5Mg alloy modified by the addition of La−Ce rare earth elements through OM, SEM, EPMA and tensile tests were investigated. The results of OM and SEM analyses indicated that primary Si particles were significantly refined from coarse block-like and irregular polygonal shapes into fine flaky shapes, while eutectic Si particles were modified from coarse and needle-like into fine and rod- or coral-like shapes with increase of La−Ce addition. The alloy exhibited the minimum primary Si particle size and the best mechanical properties with the addition of 0.3 wt.% La−Ce. The average particle size decreased from 61 to 28 μm, the ultimate tensile strength increased from 222 to 242 MPa and the elongation increased from 3.2% to 6.3%. In addition, modification mechanisms and fracture modes were explored by the means of SEM and EPMA.

Key words: Al−18Si−4Cu−0.5Mg alloy; primary Si; eutectic Si; La−Ce addition; mechanical properties

1 Introduction

Hypereutectic Al−Si alloys are important structural materials that are widely used in engine pistons, cylinder blocks, cylinder heads and motorcycle shock absorber parts due to their low density, high specific strength, low thermal expansivity, good thermal stability, high wear resistance and other advantages [1−4]. However, primary Si particles are irregular and may have plate-like and polygonal shapes, while eutectic Si particles present as needle-like in the microstructures of hypereutectic Al−Si alloys. This can lead to stress concentrations at the tips and corners of the Si phases that reduce the mechanical and cutting properties of hypereutectic Al−Si alloys [5−7]. These Si phases must be modified and refined in order to improve the practical properties of hypereutectic Al−Si alloys.

Numerous studies have been carried out on the refinement of Si phases. At present, chemical modifications using Na, Sr, P or rare earth elements have been widely used to change the morphology of Si phases as they are efficient and simple [8−11]. Many studies have reported that Sr and Na can efficaciously modify eutectic Al−Si alloys and change the morphology of eutectic Si particles from needle-like to coral-like [12,13]. Phosphorus is one of the most widely used and efficient modifiers used in conventional casting. Primary Si can be refined by adding red phosphorus, phosphate salt, Cu−P and Al−P master alloys into the alloy melt [14,15]. Recently, many studies have proven that rare earth elements, like Nd, Y, Sc, Ce and Er, can modify primary and eutectic Si. KILICASLAN et al [16] investigated the effects of Sc addition on the microstructure and mechanical properties of Al−20Si alloy. It was observed that Sc modification can not only refine the size of eutectic and primary Si but also improve the mechanical properties of Al−20Si alloy. LI et al [17] reported that with the addition of Er at a proportion of 0.5%, the primary Si particles in Al−20Si alloy were refined from

Foundation item: Project (51274245) supported by the National Natural Science Foundation of China
Corresponding author: Gao-yong LIN; Tel: +86-13507422779; E-mail: mater218@163.com
DOI: 10.1016/S1003-6326(19)65066-1

coarse polygonal, platelet- and star-like shapes to fine blocky shapes, while eutectic Si particles were modified from coarse needle-like structures to fine coral-like structures. SHI et al [18] studied the effects of Nd addition on primary Si and the wear resistance of hypereutectic Al−20Si alloy. With a 0.3% Nd addition, the average size of the primary Si decreased from 80−120 to 20−50 μm. VIJAYAN and PRABHU [19] reported that the addition of Ce to Al−14Si alloy can simultaneously refine both primary Si and eutectic Si.

Despite some investigations on the refinement of Si phases for Al−Si alloys using rare earth elements have been carried out, there is still no unified theory to explain the modification mechanisms of rare earth elements in Al−Si alloys. In the present work, there are currently no studies on the effects of La−Ce addition on the microstructure and mechanical properties of Al−18Si−4Cu−0.5Mg alloy. This study examines this relationship and discusses the mechanism of Si phases modification and the fracture modes.

2 Experimental

Hypereutectic Al−18Si−4Cu−0.5Mg alloy (wt.%) was prepared from pure aluminium, pure magnesium, Al−40Cu intermediate alloy and industrial-grade pure silicon. The modification was added in the form of misch metal (34% La, 65% Ce and 1% other rare earths). The alloy was smelted in a clay crucible in an electric resistance furnace at 820 °C. The alloy melt was degassed by adding C_2Cl_6. Subsequently, different amounts of La−Ce misch metal (0, 0.15 wt.%, 0.3 wt.%, 0.45 wt.%) were added to the alloy melt at 820 °C, and the melt was stirred and held for 15 min to ensure uniform distribution. Then, the alloy melt was poured into a grey pig iron mould at 750 °C.

Microstructures were characterized using optical microscopy (OM), scanning electron microscopy (SEM) and electron probe microanalysis (EPMA). Image Pro-Plus software (IPP) was used to analyze the size of primary Si particles. The size of primary Si molecules was characterized by the diameter of an equal-area circle. In addition, the samples were extracted with 35% HCl and 30% H_2O_2 to observe the 3D morphology of primary Si and were deeply etched with a mixed acid solution (15 mL HCl + 10 mL HF + 90 mL H_2O) to reveal the 3D morphology of eutectic Si. Samples for tensile tests were cut with a gauge length of 26 mm and a width of 3.4 mm. Tensile tests were performed at room temperature by an Instron3369 machine at a strain rate of 1×10^{-3} s^{-1}. The fracture surfaces of tensile samples were described by SEM.

3 Results and discussion

3.1 Microstructure

The OM images of the hypereutectic Al−18Si−4Cu−0.5Mg−x(La−Ce) (x=0, 0.15, 0.3, 0.45) alloys are shown in Fig. 1. Figure 2 shows the size analysis of primary Si measured by 100 grains in different fields. It can be clearly observed in Figs. 1 and 2 that the morphology of primary Si particles was modified and their size was refined with the addition of La−Ce. Figure 1(a) shows an optical micrograph of the unmodified alloy. The primary Si is present in the form of coarse block-like, needle-like and irregular polygonal shapes. According to Fig. 2(a), the maximum size of coarse primary Si was 117 μm while the average size was >60 μm. Figure 1(b) shows the microstructure of hypereutectic Al−18Si−4Cu−0.5Mg alloy containing 0.15 wt.% La−Ce. It is obvious that the coarse block-like primary Si particles were refined into fine flake-like shapes, but some irregular polygonal particles were still present. Figure 2(b) presents the size analysis of primary Si with the addition of 0.15 wt.% La−Ce. The size of primary Si particles was mainly distributed in 20−40 μm range with an average size of about 32 μm; however, the maximum size of the particles remained high at 58 μm. Figure 1(c) displays an optical micrograph of Al−18Si−4Cu−0.5Mg alloy with the addition of 0.3 wt.% La−Ce to the alloy melt. Compared with Al−18Si−4Cu−0.5Mg alloy containing 0.15 wt.% La−Ce, the primary Si particles were further refined, with an average size of about 28 μm. However, with a 0.45 wt.% addition of La−Ce, the primary Si became a little coarser (as shown in Fig. 1(d)) with an average size of 30 μm. The results demonstrate that La−Ce misch metal can not only effectively change the morphology of primary Si particles but also refine their size.

Figure 3 presents several typical 3D morphologies of primary Si particles. As shown in Fig. 3(a), primary Si without modification exhibited thick, irregular, block-like particles with coarse surfaces. Figure 3(b) shows two adjacent polyhedral primary Si particles, which were combined in the process of growth. It can be seen from Fig. 3(c) that an obvious twin groove appeared at the growth front. According to the twin plane reentrant edge (TPRE) mechanism [20,21], twin crystals at the growth front of Si crystals will create a 141° groove and a 219° peak, and the growth of Si atoms in the twin groove easily meets the interfacial free energy of silicon growth. Figure 3(d) presents a plate-like primary Si particle with a high aspect ratio. In addition, a coarse octahedron with a crack (Fig. 3(e)) transformed into an almost perfect octahedron (Fig. 3(f)) with the addition of 0.3 wt.% La−Ce. It has been reported that octahedral

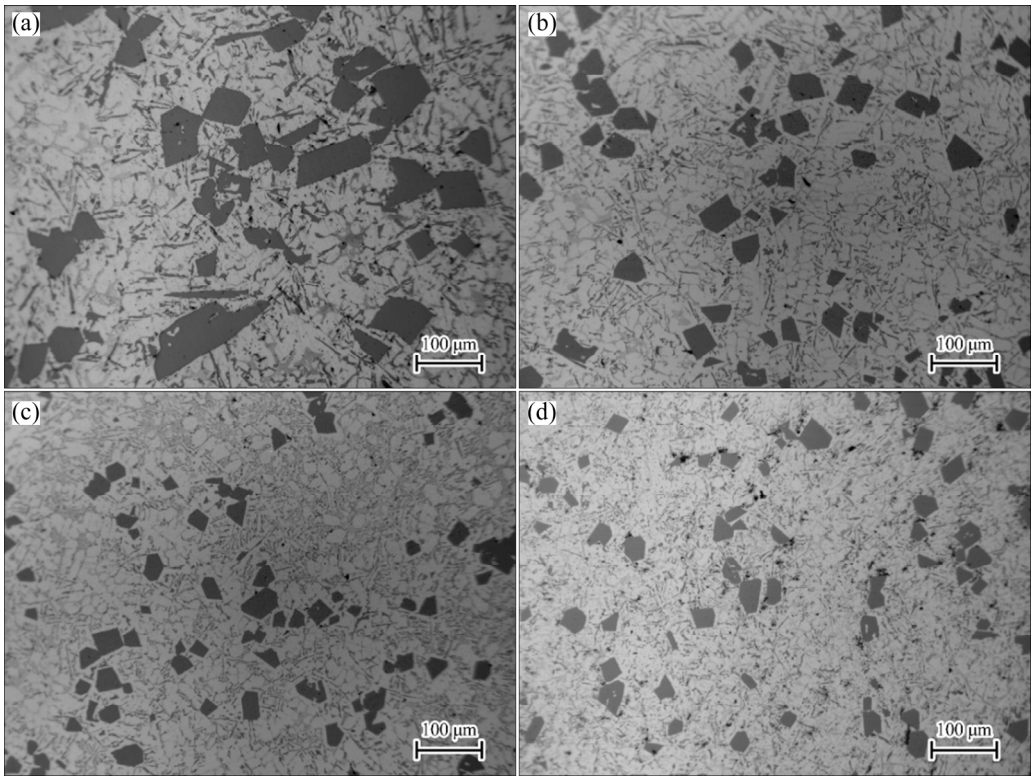

Fig. 1 Optical micrographs of Al−18Si−4Cu−0.5Mg alloy: (a) Unmodified; (b) 0.15 wt.% La−Ce; (c) 0.3 wt.% La−Ce; (d) 0.45 wt.% La−Ce

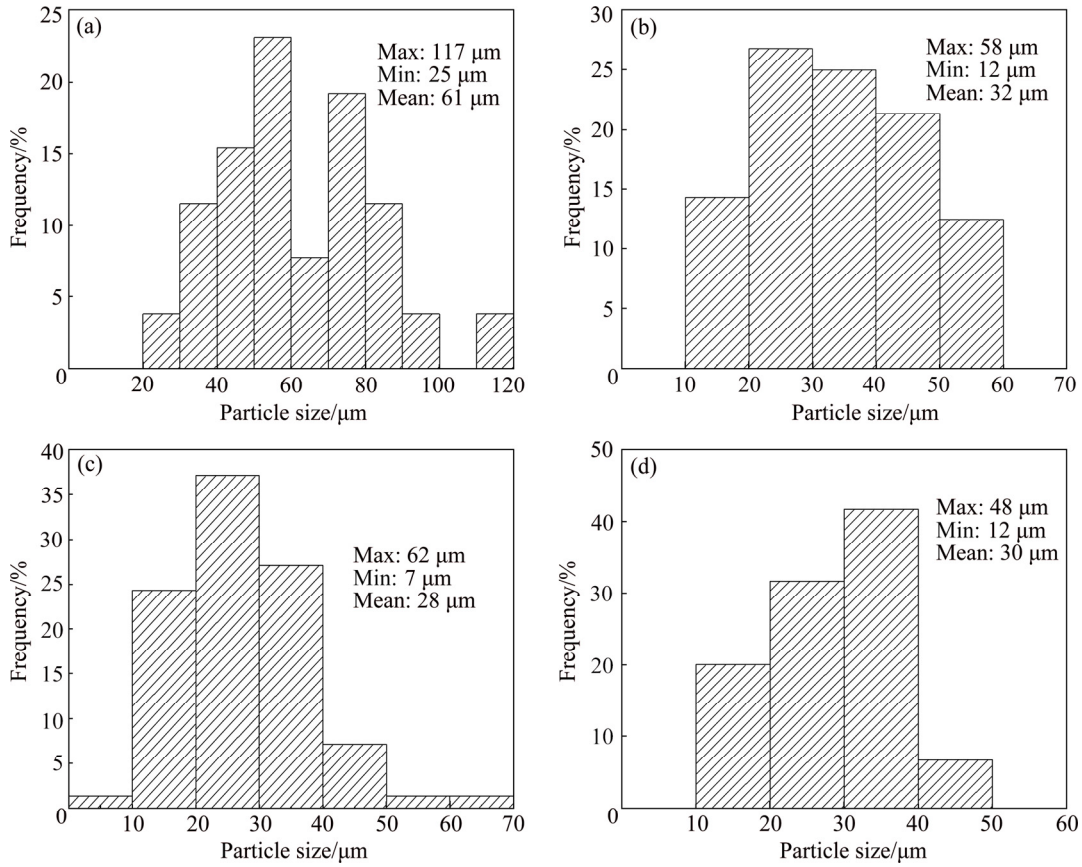

Fig. 2 Dimensional analyses of primary Si particles: (a) Unmodified; (b) 0.15 wt.% La−Ce; (c) 0.3 wt.% La−Ce; (d) 0.45 wt.% La−Ce

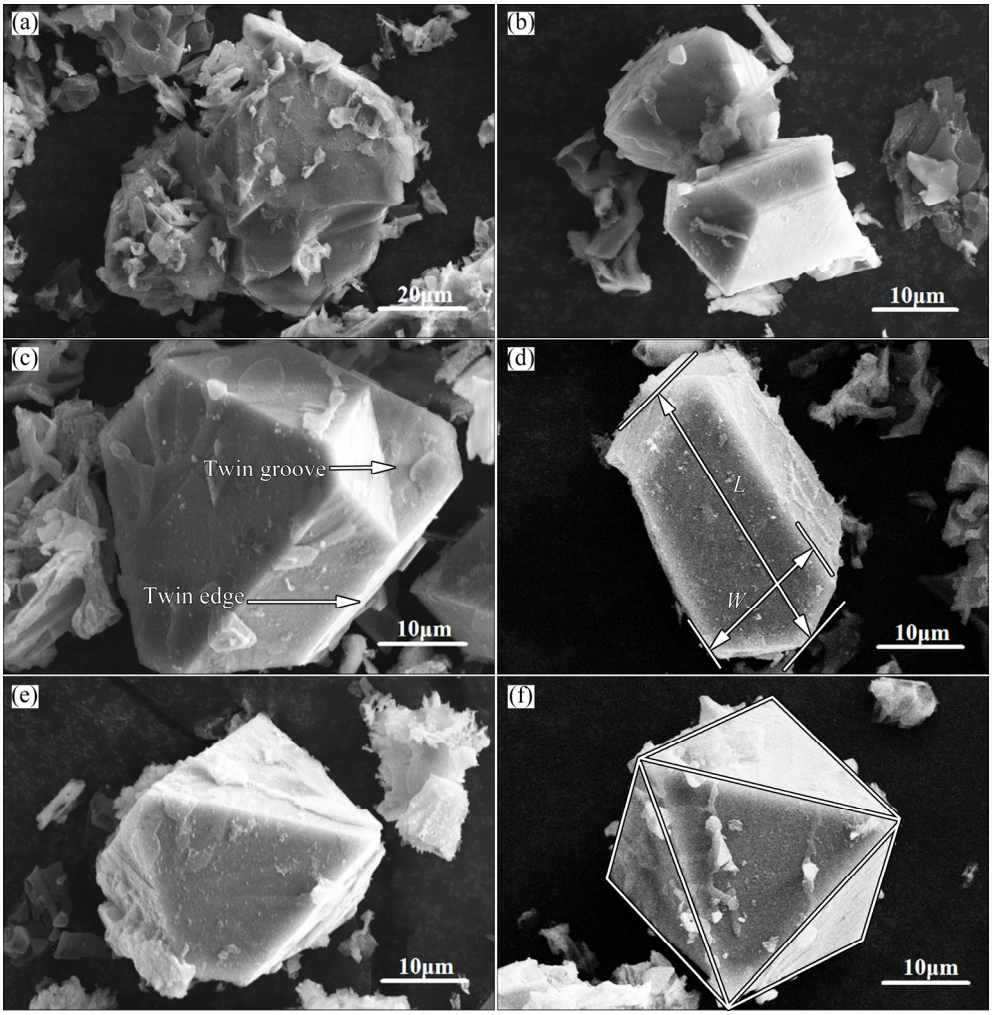

Fig. 3 Several typical 3D morphologies of primary Si particles: (a) Coarse irregular block-like; (b) Adjacent polyhedron; (c) Refined block-like with twin groove; (d) Plate-like with high aspect ratio; (e) Coarse octahedron; (f) Perfect octahedron

primary Si grows along the <100> crystal orientation in the (111) plane through a layer-by-layer growth mechanism [22].

In order to study the effects of La−Ce on eutectic Si, the microstructure was investigated by SEM (Fig. 4). Figure 4(a) shows the SEM image of hypereutectic Al−18Si−4Cu−0.5Mg alloy without La−Ce. According to EDS analysis, the bright bulky compound is mainly composed of the Al_2Cu phase and the grey, coarse, needle-like compound is eutectic Si. Figures 4(b−d) show SEM micrographs of hypereutectic Al−18Si−4Cu−0.5Mg alloy containing La−Ce at levels of 0.15 wt.%, 0.3 wt.% and 0.45 wt.%, respectively. It is clearly observed from Fig. 4 that the length of eutectic Si particles decreases significantly, while the morphology changes from coarse needle-like to fine rod-like, coral-like and dot-like structure, with the addition of La−Ce. In addition, these bulky intensive Al_2Cu phases were refined and evenly distributed in the α(Al) matrix. It is worth noting that the Al_2Cu phase becomes coarser and some eutectic Si particles transform into flake-like particles when the amount of La−Ce added is 0.45 wt.%. Figures 5(a) and (b) show the 3D morphologies of eutectic Si particles without modification and with the addition of 0.3 wt.% La−Ce, respectively. It is clear that the morphology of eutectic Si transforms from thin, needle-like and coarse lamellar structures to fine coral-like and vermicular structures. The results indicate that La−Ce misch metal can modify and refine eutectic Si in Al−18Si−4Cu−0.5Mg alloy.

Many researchers have focused on the modification mechanisms of rare earth elements in Al−Si alloys, but there is still no unified theory to explain them. A number of studies have reported that the atoms of the modifiers are enriched at the twin plane reentrant edge during solidification, which hinders the growth of Si phases (TPRE) [23]. However, the most widely accepted theory is the impurity-induced twinning (IIT) mechanism [12,24]. These studies suggest that there are many growth steps at the liquid−solid interface of Si, which makes it easier

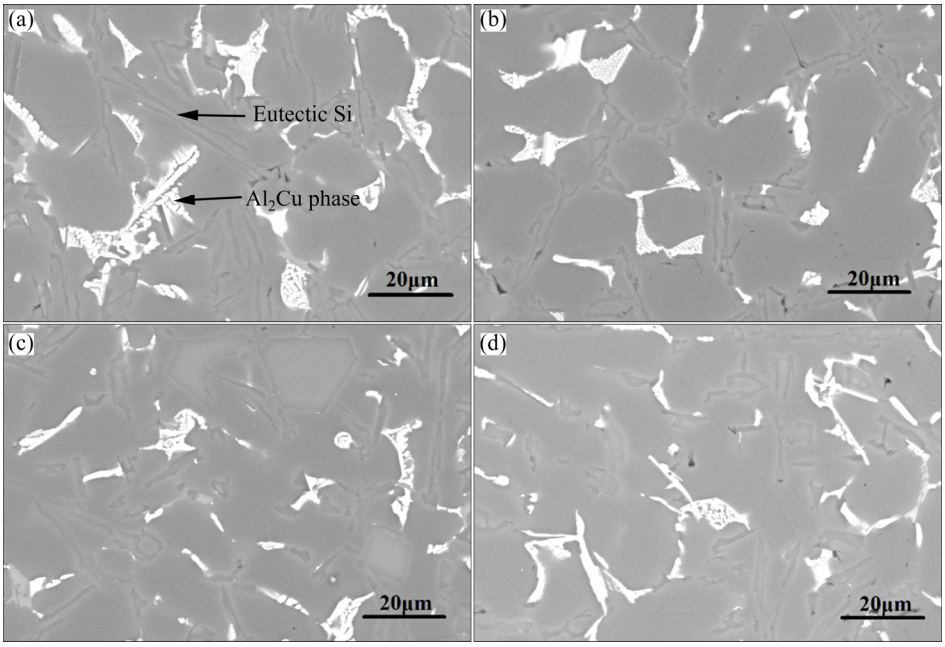

Fig. 4 SEM images of hypereutectic Al−18Si−4Cu−0.5Mg alloy: (a) Unmodified; (b) 0.15 wt.% La−Ce; (c) 0.3 wt.% La−Ce; (d) 0.45 wt.% La−Ce

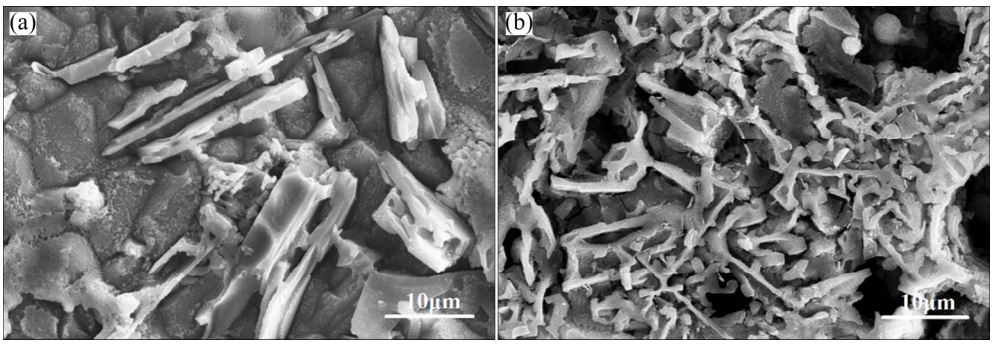

Fig. 5 3D morphologies of eutectic Si: (a) Unmodified; (b) 0.3 wt.% La−Ce

to adsorb modifier atoms than Si atoms, resulting in the refinement of Si phases. There are also other theories, such as the heterogeneous nucleation theory and composition undercooling mechanism [25].

Figure 6 shows the EPMA analysis of Al−18Si−4Cu−0.5Mg−0.45La−Ce alloy. It can be clearly observed from Fig. 6 that compounds containing La and Ce are distributed at the edge of primary Si, and these white massive compounds are rich in La and Ce elements. According to the interface step mechanism, the rare earths La and Ce, as active elements, can be absorbed during the growth steps at the liquid−solid interface of Si, resulting in stunted growth of primary Si particles. Besides, these white compounds containing La and Ce were formed when the melt temperature decreased to the eutectic reaction temperature. According to the EPMA analysis, these white compounds have a high level of Si due to the absorption of Si atoms during their formation, and they can prevent the growth of Si phases around the white compounds. In addition, LU and HELLAWELL [24] reported that if the ratio of the atomic radius of the modifier to that of silicon is close to 1.65:1, the modifier can efficiently refine the primary Si. The r_{La}/r_{Si} was 1.59:1 and the r_{Ce}/r_{Si} as 1.56:1, which are both close to 1.65:1. Therefore, primary Si can be refined efficiently by the addition of La−Ce.

During the growth of eutectic phases, La and Ce are squeezed into the growth interface by eutectic Si and α(Al) phases, resulting in an enrichment at the front of the growth interface, as shown in Fig. 7. This lowers the melting point of the solid solution, resulting in the necking and fusing of eutectic Si particles. On the other hand, this enrichment can increase the composition undercooling at the front of the growth interface, change the growth mode of eutectic Si and promote the dendritic growth of eutectic Si. Therefore, the enrichment can

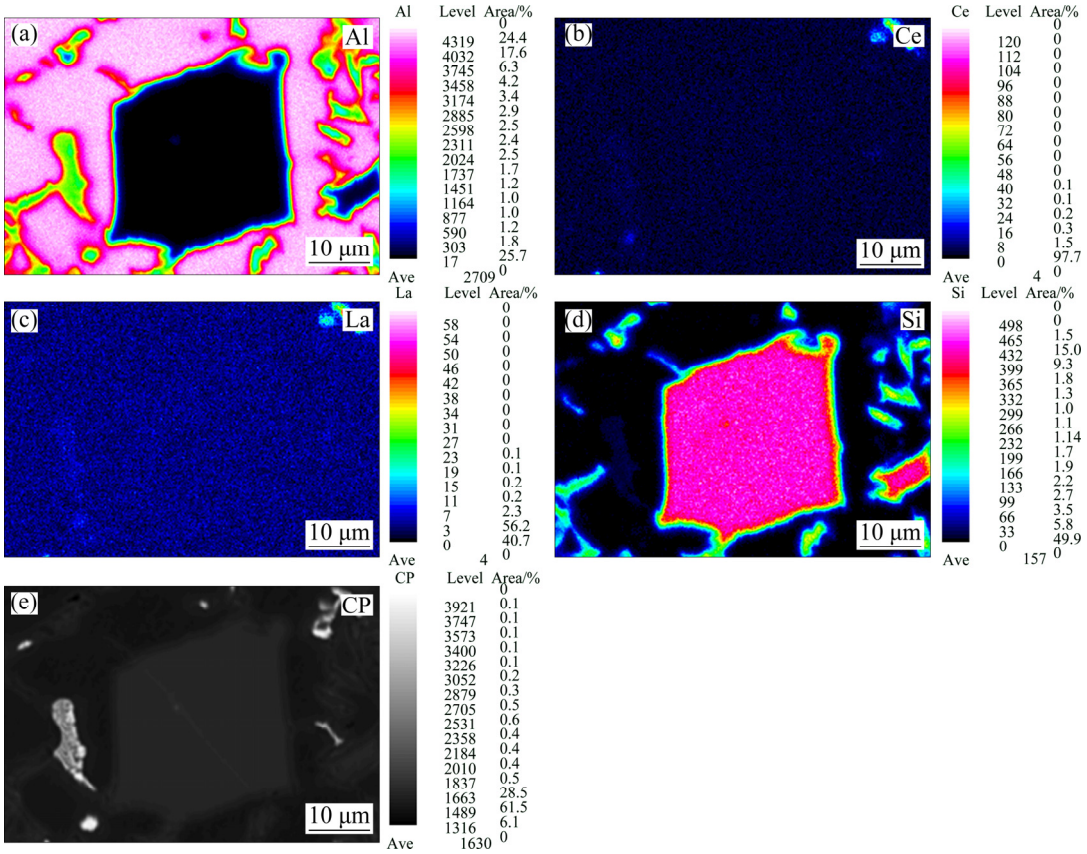

Fig. 6 EPMA analyses of Al−18Si−4Cu−0.5Mg−0.45La−Ce alloy: X-ray images of Al (a), Ce (b), La (c), Si (d) and backscattered electron image (e)

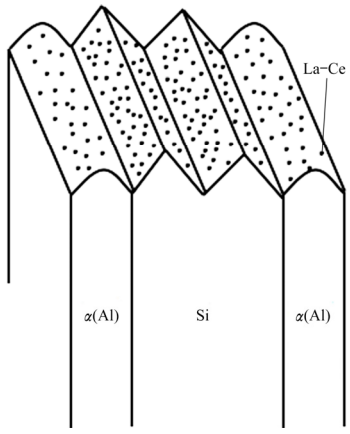

Fig. 7 Diagram of enrichment of La−Ce on eutectic Si

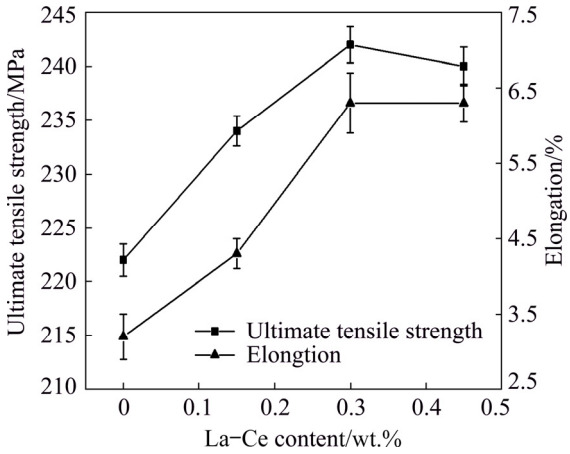

Fig. 8 Mechanical properties of hypereutectic Al−18Si−4Cu−0.5Mg alloy with different contents of La−Ce

prevent the growth of eutectic Si particles. As a result, eutectic Si particles are modified from coarse needle-like structures to fine coral-like and vermicular structures by the addition of La−Ce, as shown in Fig. 5.

3.2 Mechanical properties

Figure 8 presents the ultimate tensile strength (UTS) and elongation (El) values with the addition of various contents of La−Ce. The Al−18Si−4Cu−0.5Mg alloy with the addition of 0.3 wt.% La−Ce exhibited the best mechanical properties. The UTS increased by 9%, from 222 to 242 MPa, and the El was enhanced by 97%, from 3.2% to 6.3%. When the content of La−Ce was increased to 0.45 wt.%, there was no obvious improvement in El but a small decrease in UTS. This result agrees with the effect of La−Ce on Si particle microstructures presented in Figs. 1 and 4. The morphology and size of the Si phases play key roles in the mechanical properties of Al−18Si−4Cu−0.5Mg alloy. It has been reported that

coarse primary Si and needle-like eutectic Si particles can cause stress concentrations at the tips and corners of Si phases [5]. It is easy to induce cracks in stiff and brittle Si phases which propagate through the boundaries with the α(Al) phase [17]. The refinement of primary Si and eutectic Si can reduce stress concentrations and hinder the growth of cracks in tension. On the other hand, La and Ce can adsorb gases and remove impurities during the melting process [26], which is beneficial to the mechanical properties. Owing to the above factors, strength and plasticity are significantly improved by adding La and Ce into the alloy melt.

Figure 9 presents fractographs of hypereutectic Al−18Si−4Cu−0.5Mg alloy with different contents of added La−Ce. It is obvious that the unmodified alloy fractures as a brittle failure, as shown in Fig. 9(a). The fracture surface is mainly covered by the cleavage plane and there are many cracks in the coarse primary Si. With La−Ce addition of 0.15 wt.%, the fracture is still a brittle failure but the cracking decreases, as shown in Fig. 9(b). Furthermore, it is clearly observable from Figs. 9(c) and (d) that with additions of 0.3 wt.% and 0.45 wt.% La−Ce, respectively, there are some dimples on the fracture surface but few cracks are found in the primary Si. The fracture surface indicates that ductile failure occurs with 0.3 wt.% La−Ce and 0.45 wt.% La−Ce addition. It can be observed from Fig. 9 that the intergranular failure is mainly caused by coarse primary Si. This is because coarse, irregular, primary Si and needle-like, eutectic Si particles have sharp edges and ends, which can lead to stress concentrations and crack initiation [27]. On the other hand, coarse, irregular, primary Si has a higher level of flow stress than the α(Al) matrix and can easily fracture when the flow stress exceeds the fracture stress of the primary Si during tensile testing [28]. In addition, cracks propagate along the interface between primary Si and the α(Al) matrix, and the connection of adjacent cracks causes failure of the alloy [28]. When La and Ce are added at high proportions into alloy melt, primary and eutectic Si particles are refined and distributed uniformly. Fine primary Si is under a lower level of stress than coarse, irregular, primary Si which has sharp edges and ends. Besides, cracks more easily avoid fine primary Si particles during crack growth, which hinders their spread. Therefore, the ultimate tensile strength and elongation properties of Al−18Si−4Cu−0.5Mg alloy can be improved by adding La−Ce misch metal into alloy melt, which refines the primary Si and modifies the eutectic Si particles.

4 Conclusions

(1) La and Ce can significantly refine primary Si particles and modify eutectic Si ones. With 0.3 wt.% addition of La−Ce, the average size of primary Si particles decreases from 61 to 28 μm and the morphology transfers from coarse, block-like and irregular, polygonal shapes to fine flaky shapes, which possess the best modification effect. The morphology of eutectic Si particles is refined from coarse and needle-like shape to fine, rod-, coral- and dot-like shape with increase of La−Ce addition.

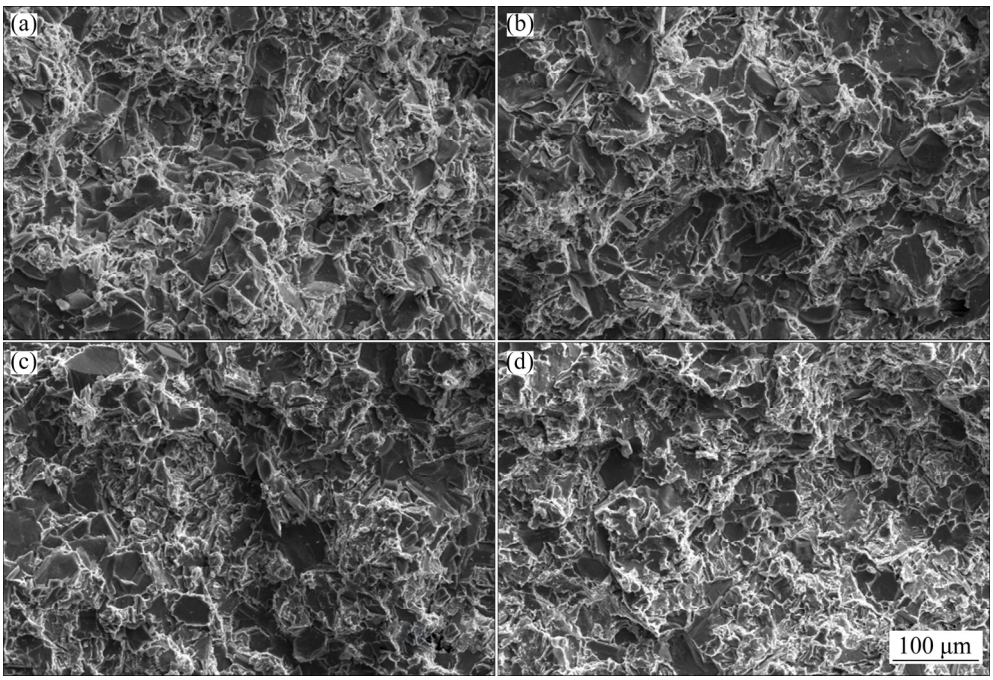

Fig. 9 Fractographs of tensile strength tests of hypereutectic Al−18Si−4Cu−0.5Mg alloy: (a) Unmodified; (b) 0.15 wt.% La−Ce; (c) 0.3 wt.% La−Ce; (d) 0.45 wt.% La−Ce

(2) La and Ce can improve the ultimate tensile strength and elongation. The ultimate tensile strength increased by 9% and the elongation by 97% with the addition of 0.3 wt.% La−Ce, due to the refinement of primary Si and modification of eutectic Si.

(3) The fracture mode transformed from brittle failure to ductile failure with increase of La−Ce addition. Alloy failures were mainly caused by coarse primary Si particles.

References

[1] EIKEN J, APEL M, LIANG S M, SCHMID-FETZER R. Impact of P and Sr on solidification sequence and morphology of hypoeutectic Al−Si alloys: Combined thermodynamic computation and phase-field simulation [J]. Acta Materialia, 2015, 98: 152−163.

[2] LIN Chong, WU Shu-sen, LÜ Shu-lin, WU He-bao, CHEN Han-xin. Influence of high pressure and manganese addition on Fe-rich phases and mechanical properties of hypereutectic Al−Si alloy with rheo-squeeze casting [J]. Transactions of Nonferrous Metals Society of China, 2019, 29: 253−262.

[3] LIN Y C, LUO S C, JIANG X Y, TANG Y, CHEN M O. Hot deformation behavior of a Sr-modified Al−Si−Mg alloy: Constitutive model and processing maps [J]. Transactions of Nonferrous Metals Society of China, 2018, 28: 592−603.

[4] KOTADIA H R, DAS A. Modification of solidification microstructure in hypo- and hyper-eutectic Al−Si alloys under high-intensity ultrasonic irradiation [J]. Journal of Alloys and Compounds, 2015, 620: 1−4.

[5] JIANG W M, FAN Z T, CHEN X, WANG B J, WU H B. Combined effects of mechanical vibration and wall thickness on microstructure and mechanical properties of A356 aluminum alloy produced by expendable pattern shell casting [J]. Materials Science and Engineering A, 2014, 619: 228−237.

[6] KANG N, CODDET P, LIAO H, CODDET C. Macrosegregation mechanism of primary silicon phase in selective laser melting hypereutectic Al–high Si alloy [J]. Journal of Alloys and Compounds, 2016, 662: 259−262.

[7] KOBAYASHI K F, HOGAN L M. The crystal growth of silicon in Al−Si alloys [J]. Journal of Materials Science, 1985, 20: 1961−1975.

[8] FATAHALLA N, HAFIZ M, ABDULKHALEK M. Effect of microstructure on the mechanical properties and fracture of commercial hypoeutectic Al−Si alloy modified with Na, Sb and Sr [J]. Journal of Materials Science, 1999, 34: 3555−3564.

[9] ZUO M, ZHAO D, TENG X, GENG H, ZHANG Z. Effect of P and Sr complex modification on Si phase in hypereutectic Al−30Si alloys [J]. Materials & Design, 2013, 47: 857−864.

[10] JIANG W, FAN Z, DAI Y, LI C. Effects of rare earth elements addition on microstructures, tensile properties and fractography of A357 alloy [J]. Materials Science and Engineering A, 2014, 597: 237−244.

[11] JING Li-jun, PAN Ye, LU Tao, PI Jin-hong, GU Teng-fei. Nucleation potency prediction of LaB_6 with E2EM model and its influence on microstructure and tensile properties of Al−7Si−0.3Mg alloy [J]. Transactions of Nonferrous Metals Society of China, 2018, 28: 1687−1694.

[12] BARRIRERO J, LI J, ENGSTLER M, GHAFOOR N, SCHUMACHER P, MAGNUS O, FRANK M. Cluster formation at the Si/liquid interface in Sr and Na modified Al−Si alloys [J]. Scripta Materialia, 2016, 117: 16−19.

[13] LIU G, LI G, CAI A, CHEN Z. The influence of Strontium addition on wear properties of Al−20wt% Si alloys under dry reciprocating sliding condition [J]. Materials & Design, 2011, 32: 121−126.

[14] SUN J F, ZHANG L, WU G H, LIU W C, HU Z H, CHEN A T. Refinement of primary Si in Al−20%Si alloy by MRB through phosphorus additions [J]. Journal of Materials Processing Technology, 2015, 225: 485−491.

[15] KYFFIN W J, RAINFORTH W M, JONES H. Effect of phosphorus additions on the spacing between primary silicon particles in a Bridgman solidified hypereutectic Al−Si alloy [J]. Journal of Materials Science, 2001, 36: 2667−2672.

[16] KILLICASLAN M F, LEE W R, LEE T H, SOHN Y, HONG, S J. Effect of Sc addition on the microstructure and mechanical properties of as-atomized and extruded Al−20Si alloys [J]. Materials Letters, 2012, 71: 164−167.

[17] LI Q, XIA T, LAN Y, ZHAN W, FAN L, LI P. Effect of rare earth cerium addition on the microstructure and tensile properties of hypereutectic Al−20%Si alloy [J]. Journal of Alloys and Compounds, 2013, 562: 25−32.

[18] SHI W X, GAO B, TU G F, LI S W. Effect of Nd on microstructure and wear resistance of hypereutectic Al−20%Si alloy [J]. Journal of Alloys and Compounds, 2010, 508: 480−485.

[19] VIJAYAN V, PRABHU K N. Effect of chilling and cerium addition on microstructure and cooling curve parameters of Al−14%Si alloy [J]. Canadian Metallurgical Quarterly, 2014, 54: 66−76.

[20] WAGNER R S. On the growth of germanium dendrites [J]. Acta Metallurgica, 1960, 8: 57−60.

[21] HAMILTON D R, SEIDENSTICKER R G. Propagation mechanism of germanium dendrites [J]. Journal of Applied Physics, 1960, 31: 1165−1168.

[22] WANG R Y, LU W H, HOGAN L M. Growth morphology of primary silicon in cast Al−Si alloys and the mechanism of concentric growth [J]. Journal of Crystal Growth, 1999, 207: 43−54.

[23] CHANG J, MOON I, CHOI C. Refinement of cast microstructure of hypereutectic Al−Si alloys through the addition of rare earth metals [J]. Journal of Materials Science, 1998, 33: 5015−5023.

[24] LU S Z, HELLAWELL A. The mechanism of silicon modification in aluminum-silicon alloys: Impurity induced twinning [J]. Metallurgical Transactions A, 1987, 18: 1721−1733.

[25] ZHANG H R, LIU Z B, LI Z Z, LI G W, ZHNAG H. Cooling rate sensitivity of re-containing grain refiner and its impact on the microstructure and mechanical properties of A356 alloy [J]. Acta Metallurgica Sinica, 2016, 29: 414−421.

[26] WANG A, ZHANG L, XIE J. Effects of cerium and phosphorus on microstructures and properties of hypereutectic Al−21%Si alloy [J]. Journal of Rare Earths, 2013, 31: 522−525.

[27] LI Q, LI B, LI J, ZHU Y, XIA T. Effect of yttrium addition on the microstructures and mechanical properties of hypereutectic Al−20Si alloy [J]. Materials Science and Engineering A, 2018, 722: 47−57.

[28] YU W, ZHAO H, WANG L, XIONG S. The influence of T6 treatment on fracture behavior of hypereutectic Al−Si HPDC casting alloy [J]. Journal of Alloys and Compounds, 2018, 731: 444−451.

添加 La−Ce 对 Al−18Si−4Cu−0.5Mg 合金显微组织和力学性能的影响

林高用[1,2]，李 坤[1,2]，冯 迪[3]，冯永平[4]，宋伟苑[1,2]，肖梦琼[1,2]

1. 中南大学 材料科学与工程学院，长沙 410083；
2. 中南大学 有色金属材料科学与工程教育部重点实验室，长沙 410083；
3. 江苏科技大学 材料科学与工程学院，镇江 212000；
4. 福建祥鑫股份有限公司，福州 350000

摘 要：通过光学显微镜、扫描电镜、电子探针和拉伸测试研究添加镧铈稀土后 Al−18Si−4Cu−0.5Mg 合金的组织演变和力学性能。光学显微镜和扫描电镜结果表明，添加镧铈稀土后初晶硅颗粒由粗大块状和不规则多边形状明显细化为细片状，共晶硅由粗长针状细化为短棒状和珊瑚状。添加 0.3%镧铈稀土时，合金具有最小初晶硅尺寸和最佳力学性能。此时，初晶硅平均尺寸由 61 μm 细化至 28 μm，抗拉强度由 222 MPa 增大到 242 MPa，伸长率由 3.2%提高至 6.3%。此外，还通过扫描电镜和电子探针探究合金的变质机制和断裂模式。

关键词：Al−18Si−4Cu−0.5Mg 合金；初晶硅；共晶硅；镧铈添加剂；力学性能

(Edited by Xiang-qun LI)